Anal. Bioanal. Electrochem., Vol. 16, No. 12, 2024, 1060-1071
https://www.doi.org/10.22034/abec.2024.719408

Analytical & Bioanalytical Electrochemistry

Full Paper

Fabrication of Thiazole Based Heterocyclic Azo Dye Modified Carbon Paste Electrode for Detection of Dopamine: A Voltammetric Study

Paalaplara H. Kusuma,[1] Chinnagiri T. Keerthikumar,[1,*] Chinnagiri T. Ramyakumari,[2] and Thippandegowdru M. Raghavendra[1]

[1]*Department of Studies in Chemistry, Davangere University, Shivagangotri, Davangere-577007 Karnataka, India*
[2]*Department of Chemistry, D R M Science College, Davangere-577002, Karnataka, India*

*Corresponding Author, Tel.: +91-9886215388
E-Mail: keerthikumarct@gmail.com

Received: 29 August 2024 / Received in revised form: 7 December 2024 / Accepted: 15 December 2024 / Published online: 31 December 2024

Abstract- A 5-[(4-phenyl-1, 3-thiazol-2yl) diazenyl] 1,3diazinane 2, 4,6trione (PTDDT) was synthesized from 2-amine-4-phenylethioazole. The synthesized PTDDT was characterized through using mass, UV-Visible, ^{1}H NMR, ^{13}C NMR, elemental analysis and FT-IR. Characterized PTDDT used as a modifier for carbon paste electrode (CPE) and was used for voltammetric detection of dopamine (DA) and uric acid (UA) using phosphate buffer solution (PBS) at pH 6.6. Many different parameters were studied such as sweep rate, varied concentration, pH study. The limit of detection is 1.056 µM for DA and 0.080 µM for UA with a limit of quantification 3.521 µM for DA and 0.267 µM for UA at PTDDT/MCPE, and it also shows good repeatability and satisfactory recovery result on real samples.

Keywords- 2-amine-4-phenylthioazole; Azo dye; Cyclic voltammetry; Carbon paste electrode; Differential pulse voltammetry

1. INTRODUCTION

Azo dyes are widely utilized class of organic compounds, illustrious for their versatility and extensive applications in science and technology. These dyes are synthesized through a direct process involving diazotization and coupling [1,2]. Which are preferred over simple

aromatic azo systems due to their greater color, brightness, stability, and fastness, are derived from heterocyclic nuclei [3,4]. The chemistry of azo dye systems is also significantly influenced by the thiazole nucleus that is present in the molecule; these moieties are also found in a large number of physiologically active compounds [5,6]. The numerous applications of thiazoles and their derivatives in various sectors have drawn ongoing interest throughout the years [7-9].

Electrochemical investigation method was chosen for the discovery of DA due to its proven advantages. Cyclic voltammetry methods are known for their selectivity, sensitivity, reliability, and cost-effectiveness [10,11]. DA is an important biogenic amine and neurotransmitter in the brain. It is a main character in different neuropsychiatric disorders such as Parkinson's disease and schizophrenia [12,13]. UA (2,6,8-trihydroxypurine) is indeed a significant nitrogenous compound found in urine [14,15]. Important level of uric acid in the blood, a situation known as hyperuricemia, can lead to various health issues including gout, kidney problems and cardiovascular diseases. Lesch-Nyhan syndrome is a rare inherited disorder that also causes high UA levels [16,17]. Generally redox reactions of DA and UA at bare electrodes are irreverscible and require high potentials. The redox reactions of DA and UA occur at similar potentials leading to poor selectivity [18-21]. Furthermore, the synthesized dye was utilize as a modifier for CPE, this electrochemical sensor used to investigate bioactive molecules using cyclic voltammetry [22,23].

Previously, we developed benzothiazole azo dyes and derivatives, azo dyes based on amino thiadizole, antipyrine-based azo dyes and aniline-based azo dyes explored their applications and those are published in different journals [24-26]. Present research work we synthesized 2-amino-4-phenylthiazole based azo dye from barbituric acid at 0-5^{0}C and was characterized by employing various kinds of spectroscopy and analytical techniques. Synthesized 5-[(4-phenyl-1, 3-thiazol-2yl) diazenyl] 1,3diazinane 2, 4,6trione (PTDDT) was used as a modifier for CPE to investigate dopamine and uric acid in voltammetric technique.

2. EXPERIMENTAL SECTION

2.1. General method for synthesis of PTDDT

2-amino-4-phenylthioazole (2 mmol) was dissolved in 4 mL of concentration HCl and quickly cooled in a salt/ice bath to 0-5^{0}C. The liquor was then added in 30 minutes to ice cold solution of nitrosylsulfuric acid (2mmol $NaNO_2$ in 3 mL H_2SO_4 at 50^{0}C). Further two hours stirring the mixture at 0˚C, this diazonium salt solution was added to the aqueous potassium hydroxide solution containing 2 mmol barbituric acid. Stirring the mixture for two more hours at the same temperature while keeping the pH between 5-6. The PTDDT was examined by thin layer chromatography using alumina-silica plates. Yellow colored solid dye was filtered out and then given a water wash, and let to dry and recrystallized with ethanol. Dye is a yellow color solid with a percentage yield of 87 and a melting point of 249^{0}C. Its FT-IR spectra are as

follows: N-H for 3360 cm^{-1}, C-H for 3088 cm^{-1}, C=O for 1664cm^{-1}, C-N for 1523 cm^{-1}, -N=N- for 1440 cm^{-1} and 803 cm^{-1} for C-S; ^{1}H-NMR (DMSO-d_6) 2.52 (S-1H, CH).7.19 (d-1H, ArH).

8.29 (d-1H, ArH). 11.88 (S-NH, 1H), and 11.59 (S. 1H, NH); MS m/z = 316.3 [M^{+1}] ion peak; ^{13}C-NMR (DMSO-d_6) 169.66 ppm, 149.92 ppm, 123.16 ppm, 112.53 ppm, 38.87 ppm. For $C_{13}H_9N_5O_3S$, C (49.52%), H (2.88%), N (22.21%), O (15.22%), and S (10.17%), the following results were obtained analytically: C 49.49; H 2.68; N 22.19; O 15.18; S 10.11.

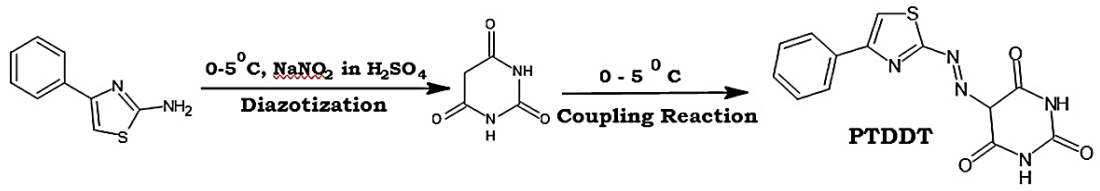

Scheme 1. Synthesis procedure for 5-[(4-phenyl-1, 3-thiazol-2yl) diazenyl] 1,3diazinane 2, 4,6trione (PTDDT)

2.2. Reagents and Chemicals

Loba Chemie was the source of the silicon oil and SD Fine Chemicals for graphite powder. 25×10^{-4} M dopamine was prepared in 0.1 M $HClO_4$ solution and 25×10^{-4} M of UA was prepared in 0.1 M NaOH were purchased form Sigma-Aldrich. Double-distilled water was utilized for prepare of 0.2 M phosphate buffer solution at different pH levels.

2.3. Apparatus

A CHI660E electrochemical workstation model was utilized to perform DPV and CV techniques. Using electrochemical cell & the electrode system consists of a counter electrode, saturated calomel reference electrode and working electrode is made of carbon paste with a diameter of 3.0 mm.

2.4. Preparation of bare carbon paste electrodes (BCPE)

To uniform BCPE, 30% silicon oil and 70% graphite powder were manually grinding an agate mortar for about half an hour to create a consistent BCPE. Weighing paper was used to smoothen the paste after it was placed into the handmade CPE.

2.5. Preparation of PTDDT/MCPE

To make a uniform azo dye-modified carbon paste electrode (MCPE), 0.05 mg of PTDDT was grind in an agate mortar with 30% silicon oil and 70% graphite powder. This procedure is around 30 minutes and the paste was filled to cavity of CPE smoothen on weighing paper.

3. RESULTS AND DISCUSSION

3.1. FT-IR Spectrum of PTDDT

The FT-IR-ALPH BRUKER IR spectrometer was obtaining the spectrum (Figure S1), which was obtained in the KBr pellets in range 4000 to 400 cm^{-1}. Absorption bands found around 3360 cm^{-1} for (N-H) group, (C=O) group 1664 cm^{-1}, (C=N) and (N=N) ranges are 1523 cm^{-1}, 1440 cm^{-1}. In addition, there were aromatic (C-H) stretching vibrations at 3088 cm^{-1} and (C-S) at 803 cm^{-1}.

3.2. Electronic absorption spectra of PTDDT

PTDDT electronic absorption spectrum (Figure S2) was obtained in the 300–600 nm range in DMSO solvent at a concentration of 2×10^{-6}M. A single absorption band in the 412 nm and this is recognized to the azo chromophore $n\rightarrow\pi*$ transition. This is because; the lone pair of electrons in the nitrogen interacts with a solvent molecule [27]. The spectrum shows that the colorant had a longer wavelength shift in aprotic solvent, a phenomenon brought by the PTDDT hydrogen atoms interacting with the solvent molecule.

3.3. ^{1}H NMR Spectrum

Using DMSO-d_6 solvent, the spectrum of PTDDT was recorded (Figure S3). PTDDT ^{1}H NMR spectra revealed significant signals at their positions, supporting the structure and being consistent with the dye predicted theoretical values. At δ 11.88 and 11.90 ppm, there are singlet protons associated with NH protons, while δ 7.5-8.3 ppm is associated with aromatic protons.

3.4. ^{13}C NMR Spectrum

The spectrum of the PTDDT (Figure S4) was recorded on an NM-ECZ 400/L1, 400MHz instrument using DMSO-d_6. The aliphatic carbon atom of the methyl group at 38.87 ppm. The signal at 112.53 ppm is connected to the azo group by the coupling component carbon atom. Aromatic carbonyl thiazole ring 123.16 ppm, 149.92 ppm, carbonyl carbon 169.66 ppm.

3.5. Mass Spectra

The PTDDT was confirmed by the mass spectra (Figure S5), which exhibit peaks at the Mass Spectra m/z = 316.3 [M^{+1}] ion peak. According to this observation, the molecular formula is $C_{13}H_9N_5O_3S$, it is apparent that the mass spectrum data constant with its molecular weight.

3.6. Electrochemical Characterization

3.6.1. Electrochemical response of potassium ferrocyanide at PTDDT/MCPE

A newly prepared solution 1 mM [$K_4Fe(CN)_6$] with supporting electrolyte in 1 M KCl was taken in electrochemical cell. Figure 1, show cyclic voltammogram (CV) for the MCPE at sweep rate 50 mVs^{-1} (solid line) and BCPE (dashed line) and MCPE (dotted line) without potassium ferrocyanide, respectively. BCPE are show slow-moving electron transfer phenomenon and a low redox peak current reaction, when PTDDT is used as modifier the electrode surface of CPE, the redox peak currents enhance significantly. This suggests that PTDDT/MCPE has enhanced electron transfer properties, likely due to improved conductivity, better active surface area, or more efficient electron exchange at the electrode interface. The higher redox peak current indicates that the modified electrode (PTDDT/MCPE) facilitates faster electron transfer kinetics, which is a good electrocatalytic activity and active surface area of BCPE and MCPE calculated using the Randles-Sevcik Equation [28].

$$I_p = 2.69\times 10^5\, n^{3/2} A\, D_0^{1/2} C_0\, \upsilon^{1/2} \qquad (1)$$

Where I_p is anodic peak current, n is number of electron transferred, D_0 is diffusion co-efficient, A is electrode active surface area (cm^2), υ is sweep rate (V/S) and C is concentration of electroactive species (mol/cm^3). Active surface area of BCPE was (0.289 cm^2) and PTDDT/MCPE was (0.443 cm^2).

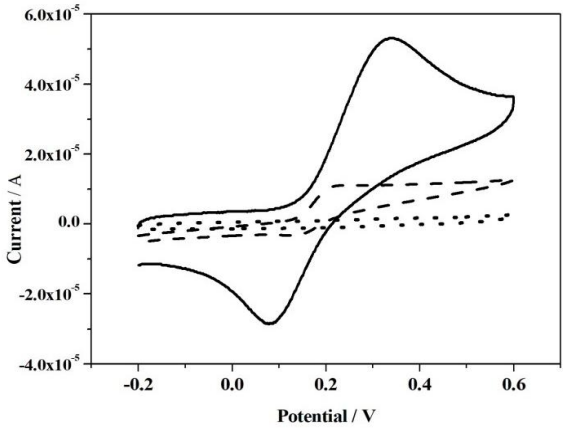

Figure 1. Cyclic voltammogram of 1 mM [$K_4Fe(CN)_6$] in 1 M KCl (dotted line), MCPE without 1mM [$K_4Fe\ (CN)_6$] (dashed line), MCPE at sweep rate 50 mVs^{-1} (solid line)

3.6.2. Effect of pH

The supporting electrolyte of pH solution at 0.2 M PBS performing an important role in influencing both the current and the E_{pa} of DA at a PTDDT/MCPE. The cyclic voltammetry results reported for 25×10^{-4} M DA at the PTDDT/MCPE with various pH solutions at a sweep rate of $50mVs^{-1}$ provide insights into the electrochemical behavior of DA. As the pH increases from 5.8 to 7.8, the E_{pa} of DA shifts in the direction of more negative values. This indicates that at higher pH levels, the oxidation process of DA becomes easier, or less energy is required for oxidation, suggesting a more efficient oxidation reaction. The shift towards a more negative

potential is commonly associated with the change in the protonation state of the electroactive species (DA in this case) and protons' involvement within the oxidation process. This behavior is depicted in Figure 2(A)**,** where the oxidation peak potential becomes more negative as pH increases. This trend is typical in electrochemical systems where proton-dependent reactions are involved and the I_{pa} is plotted against pH (Figure S6). From the graph, it was observed that the maximum I_{pa} occurred at pH 6.6. This suggests that at this pH, the electrochemical process of DA is optimized, considering these observations, the physiological pH of 6.6 was selected to do further electrochemical studies.

3.6.3. Electrochemical response of DA at PTDDT/MCPE

CVs of 25×10^{-4} M DA in 0.2 M PBS of pH 6.6 BCPE (dashed line) and PTDDT/MCPE (solid line) were recorded at a sweep rate of 50 mVs^{-1} as shown in Figure 2 (B). PTDDT/MCPE shows a well-defined redox peak for DA with E_{pa} at 0.033 V and E_{pc} at 0.018 V. Additionally, the peak current increases and the reversibility of the electron transfer process is enhanced at PTDDT/MCPE, which also has a larger surface area. The lower peak potential at PTDDT/ MCPE indicates that the electrode surface is more electrocatalytically active. This means that the materials used in PTDDT/MCPE facilitate the electron transfer process more effectively than the BCPE.

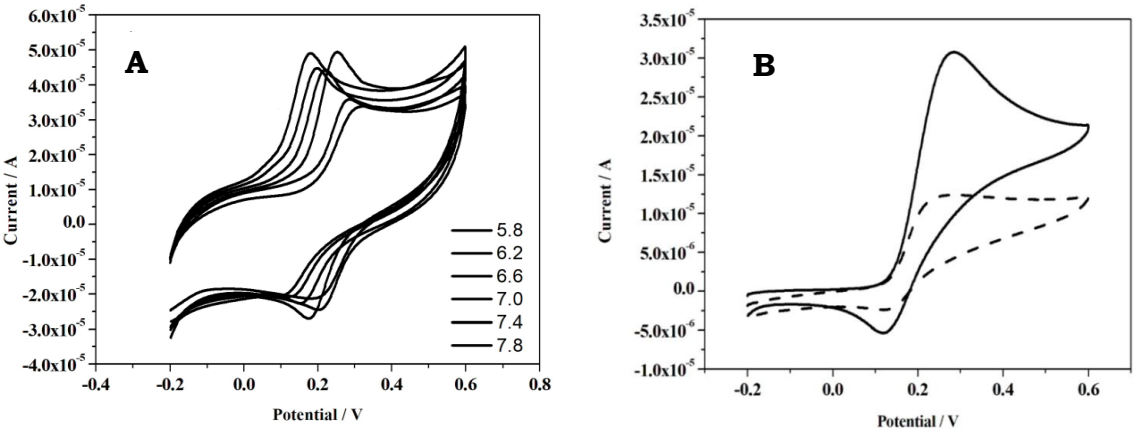

Figure 2. (A) CVs of 0.1 mM DA recorded at PTDDT/MCPE in 0.2 M PBS of different pH (5.8-7.8) having sweep rate of 50 mVs^{-1}; (B) Cyclic voltammograms dopamine in 0.2 M PBS of pH 6.6 at BCPE (dashed line) and PTDDT /MCPE (solid line)

3.6.4. Impact of sweep rate

The impact of sweep rate for DA at PTDDT/MCPE is substantially influenced by sweep rate, as shows in Figure 3(A). The I_{pc} and I_{pa} increases as the sweep rate increases from 50 to 500 mVs^{-1}. The I_{pc} of DA increase with the sweep rate increases with the Randles-Sevcik equation [29]. The E_{pa} is shifted slightly to the positive side, while the E_{pc} is shifted towards the negative side. The graph of log (υ) versus log (I_{pa}) (Figure S7), is a good linear relationship

at PTTDT/ MCPE and log I_{pa} =1.144 (logυ) – 0.482 with R^2 = 0.961. The electrode surface process is adsorption controlled.

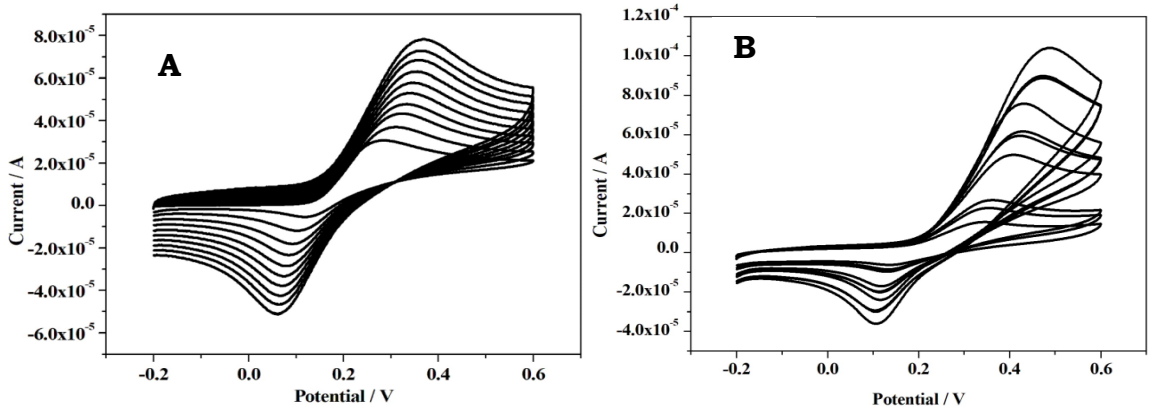

Figure 3. (A) Effect of sweep rate for DA at PTDDT/MCPE 50 mVs^{-1} to 500mVs^{-1}; (B) CVs of different concentration of DA from 100 µL to 1000 µL at PTDDT/MCPE

3.6.5. Impact of Dopamine Concentration

The PTDDT/MCPE was used to study the impact of DA concentration in a 0.2 M PBS at a pH of 6.6 is showed in Figure 3(B). Increase the concentration of DA from DA from 100 µL to 1000 µL then the redox peak current was also increases. The graph (Figure S8) shows a correlation between DA concentration and the oxidation peak current. The linear regression equation I_{pa} (A) = 0.939 (C_0µM/L) + 0.652 (R^2= 0.9940) confirmed the linearity. The calculation of LOD and LOQ were proposed by using the equation (2) and (3) respectively [30]. The calculated values of LOD and LOQ were 1.056 µM and 3.521 µM.

Table 1. Comparison of the earlier modified electrodes and PTDDT/MCPE for DA detection

Modified Electrode	**Detection Limit (µM)**	**Method**	**Ref.**
Poly (adenine) film MCNPE	0.67	CV	[31]
PA-MNPs/GCE	0.14	EIS	[32]
Poly Alizarin sodium sulfonate modified Carbone nanotube paste electrode	7.8	CV	[33]
GQDs@MWCNTs	0.095	DPV	[34]
Rhodamine B/CPE	3.99	CV	[35]
HRP–MWCNTs–SiSG/Poly (Gly)/CPE	0.6	DPV	[36]
PTDDT/MCPE	0.10	CV	Present work

CV- Cyclic voltammetry; EIS-Electrochemical impedance spectroscopy; CPE – Carbon paste electrode, GCE Glassy carbon electrode; MCNPE- Modified carbon nanotube paste electrode; DPV- Differential pulse voltammetry

$$LOD = 3S/M \quad (2)$$

$$LOQ = 10S/M \quad (3)$$

Where S represents for the standard deviation, M represents the slope determined from the calibration plot. Additionally, Table 1 was contrasted with other electrodes for the detection of DA.

3.6.6. Electrochemical response of Uric acid at PTDDT/MCPE

CVs of UA in 0.2 M PBS of pH 6.6 at BCPE (dashed line) and PTDDT/MCPE (solid line) was recorded at a sweep rate 50 mVs^{-1} Figure 4(A). The (PTDDT/MCPE) would exhibit a significantly increased peak current compared to the BCPE. This increase is recognized to the enhanced electrochemical activity and higher surface area provide by the PTDDT/MCPE. At BCPE the CV of UA (dashed line) shows an E_{pa} at 0.36 V. At PTDDT/MCPE well distinct oxidation wave of UA was obtained with an enhance of the I_{pa} (solid line). The E_{pa} occurs at 0.39 V, which is slightly higher than that at the BCPE. The peak currents are greatly enhanced compared to those at the BCPE, showing improved sensitivity and better catalytic effect at the PTDDT/MCPE.

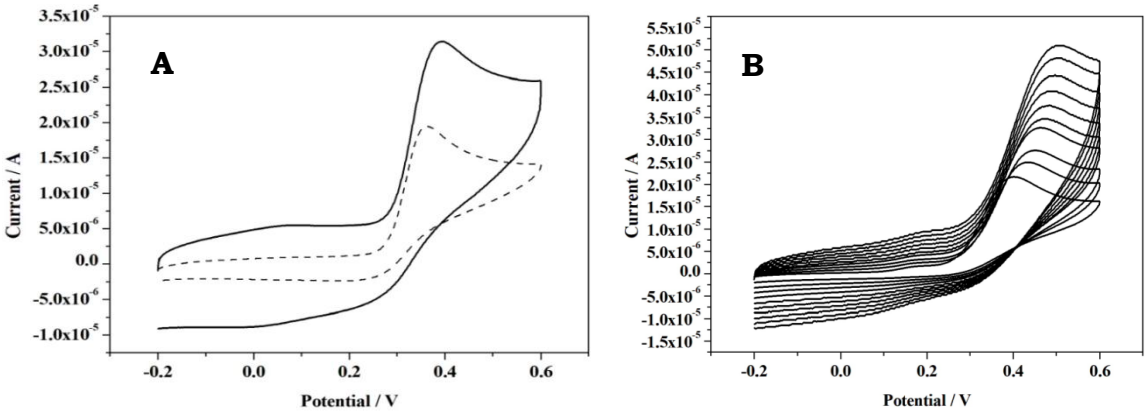

Figure 4. (A) CVs of UA in 0.2 M PBS of pH 6.6 at BCPE (dashed line) and PTDDT/ MCPE (solid line); (B) Variation of sweep rate for UA from 50 mVs^{-1} to 500 mVs^{-1} at PTDDT/ MCPE

3.6.7. Impact of UA sweep rate

UA cyclic voltammograms were collected at different sweep rates. According to Figure 4(B) the sweep rate significantly affects the current of UA at PTDDT/MCPE. The I_{pa} increases sweep rate also increase from 50 mVs^{-1} to 500 mVs^{-1}. It is evident that when sweep rates increased, oxidation peak currents gradually increased and the highest potential oxidation shifted to positive direction. The graph (Figure S9) shows good linear relationship of PTTDT/MCPE is log I_{pa}= 0.580 (logυ)-0.244 with correlation coefficient of R^2=0.912 at PTDDT/MCPE the electrode surface process is controlled by adsorption.

3.6.8. Impact of UA Concentration

Figure 5(A) presents that the PTDDT/MCPE was used to study the concentration impact of UA in 0.2 M PBS at a pH-6.6. Increasing the concentration of UA from 10 µM to 100 µM

I_{pa} was also increases. The graph (Figure S10) of the calibration plot, I_{pa} versus concentration of UA, linear regression equation, $I_p(\mu A)$ =1.51927 ($C_0\mu M/L$) + 1.1832 R^2 = 0.99653. It was revealed that the calculated LOD values were 0.0804 µM and the LOQ values was 0.2680 µM, respectively.

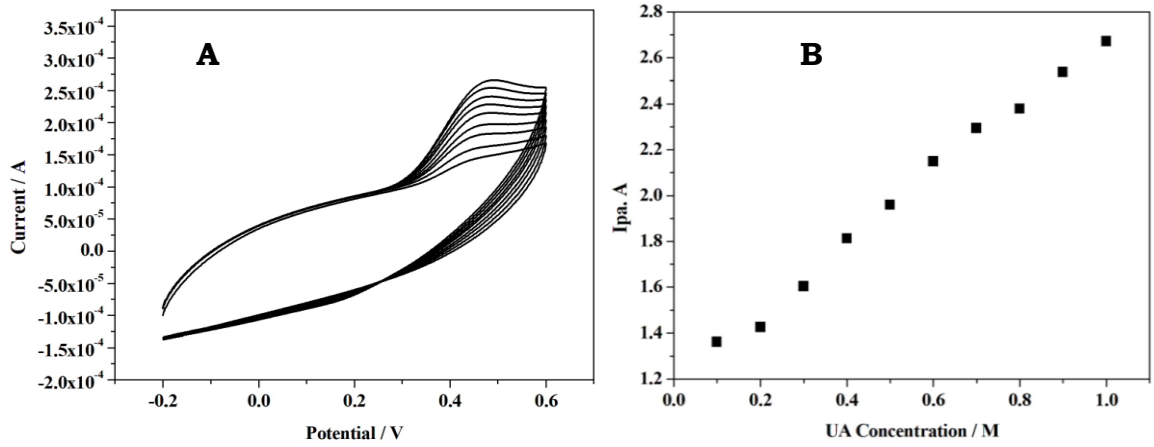

Figure 5. (A) Cyclic voltammogram of UA at different concentration 10 to 100 µL in 0.2 M PBS; (B) I_{pa} versus UA of concentration

3.6.9. Simultaneous determination of DA and UA at cyclic voltammetry

CV for the solution containing DA and UA mixture at 50 mVs^{-1} sweep rates in a pH 6.6 PBS is displayed in Figure 6(A). It displaying two distinct anodic peaks, the maximal values of DA and UA oxidation can be distinguished by PTDDT/MCPE. The variation in the potentials for DA and UA from peak to peak was 231 mV. The E_{pa} of UA and DA were nearly similar, The PTDDT/MCPE can distinguish between the DA and UA oxidation peak potentials to determine simultaneous and individually [37,38].

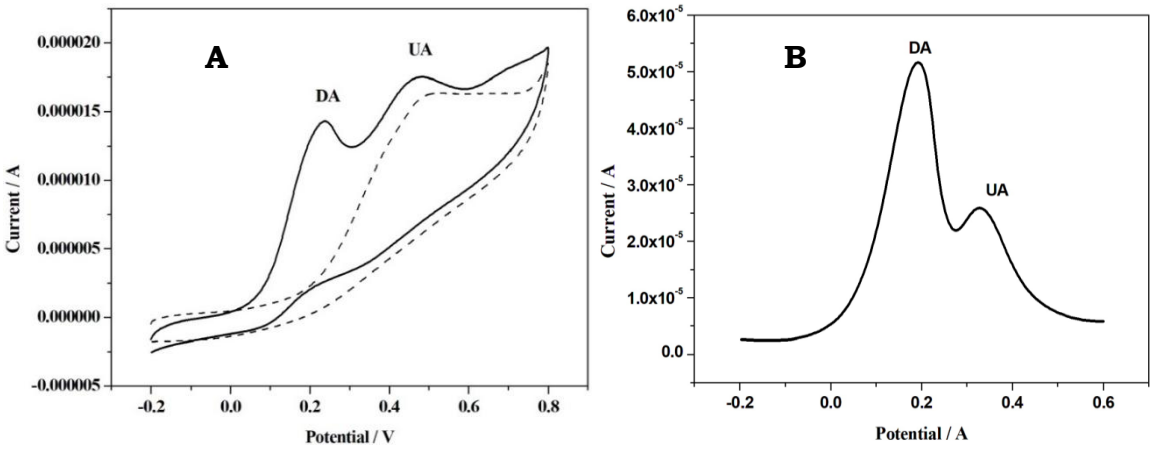

Figure 6. (A) Simultaneous determination of 10 µM DA and 10µM UA at BCPE (dashed line) PTDDT/MCPE (solid line) in 0.2 M PBS of pH 6.6 by CV at 50 mVs^{-1}; (B) Simultaneous determination of 10 µM DA and 10µ M UA at PTDDT/MCPE in PBS of pH 6.6 by DPV

3.6.10. Simultaneous determination at Differential Pulse Voltammetry (DPV)

Simultaneously determination 25×10^{-4} M DA and 25×10^{-4} M UA at PTDDT/MCPE at pH 6.6 in 0.2 M PBS. The differential pulse voltammetric approach was used to resolve this combination of two samples. The oxidation peaks were DA and UA, obtained at 240 mV and 370 mV, respectively [39]. There was a 130 mV difference between the DA and UA peaks is more than sufficient to detect individually and simultaneously as shown in Figure 6(B).

3.6.11. Real sample analysis

A commercially available dopamine hydrochloride injection was used to show the delivered sensor sensitivity, which contained a specified concentration of 40 mg/mL of DA. The injectable solution in 0.2 M PBS with a pH of 6.6, and possibly mentioning a concentration or dissolving of 25×10^{-4} M [40,41]. The conventional addition technique was applied to analyze the sample and measure the amount of DA there in the pharmaceutical formulation. The spiked sample recoveries ranged from 93.3% to 118%. Therefore, the suggested sensor could work well with actual sample analysis, yielding reliable results shown in Table 2.

Table 2. DA determination in an injectable sample (n=3)

Sample	**Labelled**	**Added (µM)**	**Found (µM)**	**Recovery (%)**
DA injection	1	1	1.03	103
	2	2	2.36	118
	3	3	2.80	93.3

4. CONCLUSION

In this study, we synthesized PTDDT and characterized, it through the spectral techniques FT-IR, 1HNMR, 13CNMR, UV-Vis, mass and elemental analysis. The PTDDT was used as modifier for CPE. Electrochemical studies of DA and UA was investigated by using 0.2 M PBS at PTDDT/MCPE. Furthermore, pH study, impact of sweep rate and impact of concentration dopamine was evaluated than LOD is 1.056 µM and LOQ is 3.521 µM both DA and UA. The activity of electrochemical reactions reveals the oxidation process of dopamine in PBS at pH 6.6, where the similar number of electrons (e^-) and protons (H^+) were involved in the reaction. The PTDDT/MCPE demonstrated remarkable selectivity towards detection of DA and UA, the peak-to-peak potential variation was 130 mV and this was satisfactory to determine. The distinction between the DA and UA oxidation peak potential the variation however significant enough to use DPV and CV to measure UA and DA individually and simultaneously. The application of analysis the PTDDT/MCPE was also shown for determining real sample is yielding good recovery. Overall, the MCPE, often used in

electrochemical analysis is a material or device used for the sensitive and selective determination of biological molecule.

Declarations of interest

The authors declare no conflict of interest in this reported work.

REFERENCES

[1] S. Benkhaya, S. M'rabet, and A. El Harfi, Heliyon 6 (2020) 234.
[2] V.J. Keshavayya, I. Pushpavathi, C.T. Keerthikumar, M.R. Maliyappa, and B.N. Ravi, Struct. Chem. 31 (2020) 1317.
[3] Z.A. Siddiqui, B. Chaudhary, S. Tewari, N. Sekar, and S. More, Textile Dyes and Pigments (2022) 225.
[4] X. Zheng Zhao, W. Miao, and W. Huang, Dyes and Pigments 187 (2021) 109087.
[5] S.H. Alotaibi, A.S. Radwan, Y.K. Abdel-Monem, and M.M. Makhlouf, Spectrochim. Acta A 205 (2018) 364.
[6] M. Yahya, R. Metin, B. Aydıner, N. Seferoğlu, and Z. Seferoğlu, Anal. Sci. 39 (2023) 829.
[7] B.N. Ravi, J. Keshavayya, and S.V. K. Kandgal, J. Mol. Struct. 1204 (2020) 127493.
[8] N. El Guesmi, A.Y. Khormi, A.S. Alzahrani, B.H. Asghar, S. Kaya, K.P. Katin, and A.M. Farag, J. Mol. Liq. 383 (2023) 122119.
[9] S. Harisha, J. Keshavayya, B.K. Swamy, S.M. Prasanna, C.C. Viswanath, B.N. Ravi. J. Mol. Liq. 271 (2018) 976.
[10] S.A. H Ta'alia, E. Rohaeti, B.R. Putra, and W.T. Wahyuni, Results in Chem. 6 (2023) 101024.
[11] N. Özdemir, and E. Biçer, Russian J. Electrochem. 53 (2017) 486.
[12] Li, Ying, Int. J. Electrochem. Sci. 10 (2015) 7671.
[13] N.M. Mallikarjuna, J. Keshavayya, King Saud Univ. Sci. 32 (2020) 251.
[14] K.R. Mahanthesha, B.E. Kumara Swamy, and U. Chandra, JETIR 5 (2018) 520.
[15] H. Abdalkarem, M.S.A. Yashıl, and İ.O. Koçoğlu, Monatshefte fur Chemie 155 (2024) 663.
[16] D.P. Prashanth, J.G. Manjunatha, K.P Moulya, C. Raril, S.A.A. Mohammad, Monatshefte fur Chemie 155 (2024) 345.
[17] S. Chitravathi, and N. Munichandraiah, J. Electrochem. Soc. 162 (2015) B163.
[18] D.G. Dilgin, K. Vural, S. Karakaya, Y. Dilginz, Monatshefte fur Chemie 155 (2024) 81.
[19] M. Asha, J.G. Manjunatha, K.P. Moulya, S.A. Aldossari, M.S. Mushab, Monatshefte Chemie 155 (2024) 37.
[20] S.D. Sukanya, S. Kumar, and B.E. Swamy, Anal. Bioanal. Electrochem. 12 (2022) 1114.

[21] K.R. Mahathesha, B.E.K. Swamy, U. Chandra, T.V. Sathisha, S. Sarojini, and K.V.K. Pai, Anal. Bioanal. Electrochem. (2013) 130.
[22] A. Abdel-Reroof, and M. Ahmed, J. Electrochem. Soc. 166 (2019) B 948.
[23] A. Ahammad, A.S. Ahammad, T. Islam, M. M Hasan, M.I. Moumder, R. Karim, N.O. Dhikari, and D.M. Kim, J. Electrochem. Soc.165 (2018) B174.
[24] C.T. Keerthikumar, J. Keshavayya, T. Rajesh, S.K. Peethambar, Int. J. Pharm. Sci. (2013) 0975.
[25] C.T. Keerthi Kumar, J. Keshavayya, and J. Rajesh, Int. J. Edu. Tech. Sci. 4 (2017) 996.
[26] C.T Keerthi Kumar, J. Keshavayya, S.K. Peethambar, Chem. Rev. Lett. 5 (2016) 59.
[27] J. Keshavayya, J. Mol. Struct.1186 (2019) 404.
[28] Y. Wei, Y. Liu, Z. Xu, S. Wang, B. Chen, D. Zhang, and Y. Fang, Int. J. Anal. Chem. 1 (2020) 8812443.
[29] G.K. Jayaprakash, B.E.K Swamy, B.N. Chandrashekar, and R. Flores-Moreno, J. Mol. Liq. 240 (2017) 395.
[30] P. Zhi, Colloids Surf. A 635 (2022) 128083.
[31] N.S. Prinith, J.G. Manjunatha, and C. Raril, Anal. Bioanal. Electrochem. 11 (2019) 742.
[32] S. Chandra, K. Arora, and D. Bahadur, Mater. Sci. Eng. B 177 (2012) 1531.
[33] N. Hareesha, J.G. Manjunatha, C. Raril, and G. Tigari, ChemistrySelect 4 (2019) 4559.
[34] S.K. Arumugasamy, S. Govindaraju, and K. Yun, Appl. Surf. Sci. 508 (2020) 145294.
[35] T. Thomas, R.J. Mascarenhas, and B.K. Swamy, J. Mol. Liq. 174 (2012) 70.
[36] P. Raghu, T.M. Reddy, P. Gopal, K. Reddaiah, and N.Y. Sreedhar, Enzyme Microb. Technol. 57 (2014) 8.
[37] S. Chun-Hao, C. Sun, and Y. Liao, ACS Omega 2 (2017) 4245.
[38] Q. A Moallem, and H. Beitollahi, Microchem. J. 177 (2022) 107261.
[39] H. Beitollahi, M. Hamzavi, M. Torkzadeh-Mahani, M. Shanesaz, and H.K. Maleh, Electroanalysis 27 (2015) 524.
[40] H. Zhang, and S. Liu, J. Alloys Compd, 8 (2020) 155873.
[41] M.A. Abdel-Aziz, H. HamdyHassan, and H.A. Badr Ibrahim, ACS Omega 7 (2022) 34127.